Supporting Information

Intermittent beading in fiber composites

Israel Greenfeld[*,‡], Wenyong Zhang[‡], XiaoMeng Sui, and H. Daniel Wagner[*]

Department of Materials and Interfaces, Weizmann Institute of Science, Rehovot 76100, Israel

‡These authors contributed equally to this work.

*Corresponding authors e-mail addresses:

green_is@netvision.net.il (I. Greenfeld),

Daniel.Wagner@weizmann.ac.il (H.D. Wagner)

Contents:

Plateau-Rayleigh instability and beads formation

Intermittent beading was obtained by taking advantage of the Plateau-Rayleigh liquid instability phenomenon in a cylindrical liquid film. The spontaneous formation of evenly spaced drops on a fiber coated by a liquid layer, and the shape of the drops, are widely described in the literature, for example in [1]. These are briefly discussed here for completeness and in the context of the simulation of the beads frequency, shape and dimensions.

S1. Plateau-Rayleigh instability

Small curvature perturbations in a cylindrical liquid film cause pressure gradients and liquid flow driven by surface tension, such that the liquid surface area and surface energy are minimized, as first perceived by Plateau in 1873 [2]. The surface wavelength (and consequently the drop size) is determined by the fastest growing instability mode, as shown by Lord Rayleigh in 1873-1879 [3].

Starting with a cylindrical film of thickness e_0 and radius r_0, coated over a fiber of radius b, the liquid surface is modulated by the instability with local thickness e and radius r, resulting in varying curvature along the x axis (Figure S1).

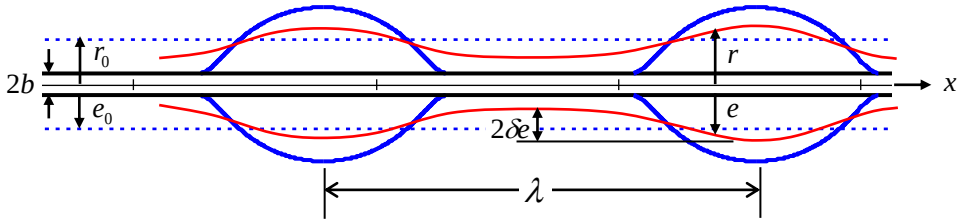

Figure S1. Plateau-Rayleigh instability. *The fiber radius is* b. *The dashed lines indicate the initial cylindrical liquid coating, with radius* r_0 *and thickness* e_0. *The red wavy curves represent a modulation of wavelength* λ *and amplitude* δe *of the liquid surface as a result of instability, with local radius* r *and thickness* e. *The blue curves represent the final stable drops.*

For weak slopes, the two orthogonal curvatures of the liquid surface at point xr are r^{-1} in the plane perpendicular to x and $-d^2r/dx^2$ in the plane xr. The local pressure difference between the liquid and the surrounding medium is the product of the surface tension γ and the surface curvature (Laplace equation):

$$\Delta p = \gamma\left(\frac{1}{b+e} - \frac{d^2e}{dx^2}\right) \qquad \text{(S1)}$$

where we substituted $r = b + e$. For a periodic surface modulation of wavelength λ, if the wavelength is larger than the perimeter of the cylindrical coating, that is $\lambda > 2\pi r_0$, the pressure is higher at the narrow region (small r) of the wavy surface than in the wide region (large r). This pressure gradient further drives the liquid from the narrow regions to the wide regions, creating drop-like surfaces. The process is unstable, as a small disturbance in the original cylindrical shape is sufficient to create an initial pressure gradient, which forces liquid flow that increases the amplitude of the surface modulation, further increasing the pressure gradient, eventually evolving the surface into stable drops.

Given the volumetric force (the pressure gradient), $f = d\Delta p / dx$, the flow rate in the x direction, per unit length of the film circumference, is proportional to f, and is expressed by Poiseuille's law for thin liquid films:

$$Q = \frac{e^3 f}{3\eta} \tag{S2}$$

where η is the liquid viscosity. Inertia and gravity are negligible for the size scale involved. The effect of gravity can be assessed by comparing the Laplace pressure induced by surface tension and the hydrostatic pressure due to gravity. The balance between these pressures yields the capillary length, a size scale for which the two effects are comparable. The capillary length of the liquid epoxy is $\sqrt{\gamma / \rho g} \cong 1.5\,\text{mm}$, ($\gamma \cong 40\,\text{mN/m}$ is the epoxy surface tension, $\rho \cong 1.9\,\text{g/mL}$ is its density, and g is gravitation), more than an order of magnitude larger than typical drops formed in our study, and therefore the effect of gravity can be neglected for such micro-scale beads. Also neglected are viscoelastic effects, which can be ignored when the epoxy is at liquid state, when cross-linking by curing has not yet started.

For thin films, if the film thickness changes at a rate $\partial e / \partial t$, the flow rate will change over a distance dx by $(\partial e / \partial t)dx$, and therefore volume conservation is maintained by:

$$\frac{\partial Q}{\partial x} = -\frac{\partial e}{\partial t} \tag{S3}$$

Assuming sinusoidal surface modulation of the form $\delta e \cos qx$, where δe is the modulation amplitude and $q = 2\pi / \lambda$ is its wave number (Figure S1), and combining equations (S1)-(S3), we obtain the differential equation of the instability:

$$\frac{d\delta e}{dt} = \frac{\delta e}{\tau} \tag{S4}$$

where the characteristic time constant τ is:

$$\tau = \left[\frac{\gamma e_0^3}{3\eta r_0^2} q^2 \left(1 - q^2 r_0^2\right) \right]^{-1} \tag{S5}$$

where $r_0 = b + e_0$. When $qr_0 < 1$, that is the modulation wavelength is larger than the initial coating circumference ($\lambda > 2\pi r_0$), the modulation amplitude diverges with time ($\delta e = \exp(t/\tau) - 1$), hence the instability.

For each wavelength the instability has a matching characteristic time τ, but the fastest one is dominant over all the others, and therefore the modulation wavelength is that which minimizes the time constant τ, that is $q = (\sqrt{2} r_0)^{-1}$ or:

$$\lambda = 2\sqrt{2}\pi r_0 \tag{S6}$$

The corresponding time constant is:

$$\tau = \frac{12\eta r_0^4}{\gamma e_0^3} \tag{S7}$$

The characteristic growth time of the liquid instability is very sensitive to the liquid coating thickness e_0. For example, using $\eta = 13$ Pa s and $\gamma = 40$ mN/m for liquid epoxy, the assessed growth times for our study range from less than a second for the thickest coating to tens of seconds for the thinnest coating. For practical coating thicknesses of several microns or higher, the beads formation time should be typically less than 1 s.

The flow into drops continues until the remaining liquid film between the drops becomes very thin, and balance is reached between the van der Waals forces and the forces induced by the Plateau-Rayleigh instability, as predicted by theory [1]. However, this effect accounts for film thickness of the order of 10 nm [1], whereas our measurements show a thickness of 100-200 nm, a discrepancy that may be explained by the curing of the epoxy resin. When the film thickness becomes very thin, the flow's characteristic time is in the order of hours, similar to the epoxy curing time. The characteristic time of the flow in a thin film can be derived by the following dimensional approach. The pressure difference between the film and a neighboring drop is approximately γ / b (equation (S1)), assuming the drop radius is much larger than the fiber radius. Therefore, the flow force f (the pressure gradient) along a film length of order λ is $\gamma/(b\lambda)$, and the Poiseuille's velocity is $V = Q(f)/e$ (equation (S2)). The characteristic time scales as λ / V (to within a numerical prefactor):

$$\tau \approx \frac{\eta b r_0^2}{\gamma e^2} \qquad \text{(S8)}$$

where we substituted $\lambda \propto r_0$ (equation (S6)). The accurate calculation yields a numerical prefactor $3\pi^2$. For example, in the case of a fiber of radius $b = 10\,\mu\text{m}$, whose initial epoxy resin coating is of radius $r_0 = 20\,\mu\text{m}$, the characteristic time of the flow in a film of thickness $e = 100\,\text{nm}$ between the drops is about 1 hour.

S2. Bead shape

A drop created by the liquid film instability eventually stabilizes when the surface tension and the pressure reach equilibrium. Consider a liquid drop of diameter D deposited on a fiber of diameter d, and the forces acting on a drop segment extending from $x = 0$ to x along the fiber axis (Figure S2). At the liquid-fiber end contact ($x = 0$), the surface tension force f_1 projected on the x axis is $-\pi d\gamma \cos\theta_E$, where θ_E is the liquid-fiber contact angle. At the right side of the segment, the surface tension force f_2 projected on the x axis is $2\pi r\gamma \cos\theta$, where θ is the drop slope angle at point x, r. The force f_3 due to the pressure difference Δp between the drop and the surrounding medium is $-\Delta p\pi(r^2 - d^2/4)$.

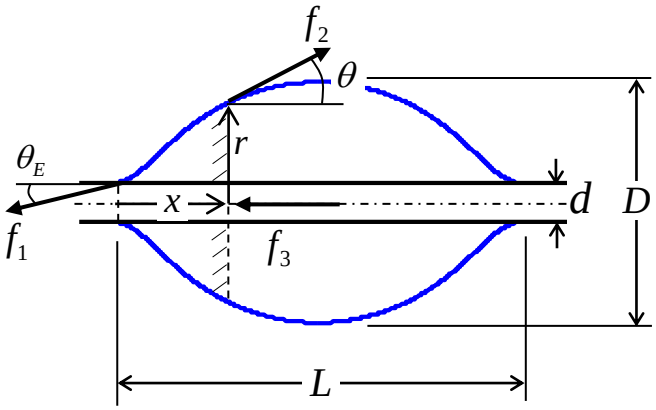

Figure S2. Shape of a liquid drop on a fiber. *Forces acting on a drop segment (marked by dashed lines):* f_1 *and* f_2 *are forces due to surface tension, and* f_3 *is a force due to pressure difference.*

Force equilibrium yields:

$$2r\cos\theta - \frac{\Delta p}{4\gamma}(4r^2 - d^2) = d\cos\theta_E \tag{S9}$$

The term $\Delta p/\gamma$ is obtained at the highest point where $\theta = 0$ and $r = D/2$:

$$\frac{\Delta p}{4\gamma} = \frac{D - d\cos\theta_E}{D^2 - d^2} \tag{S10}$$

Note that the term $\Delta p/\gamma$ is equal to the drop surface curvature (Laplace law). Using the relationship $\cos\theta = [1+(dr/dx)^2]^{-1/2}$, we obtain the differential equation that describes the drop geometry [1]:

$$\frac{2r}{\sqrt{1+(dr/dx)^2}} - (D - d\cos\theta_E)\frac{4r^2 - d^2}{D^2 - d^2} = d\cos\theta_E \tag{S11}$$

The boundary condition is $r = d/2$ at $x = 0$. The variables x, r in this equation can be separated, and then integrated (numerically) for given parameters D, d, θ_E, yielding the drop contour $x(r)$:

$$x(r) = \int_{d/2}^{r} \left\{ \left[\frac{2r(D^2 - d^2)}{D(4r^2 - d^2) + d(D^2 - 4r^2)\cos\theta_E} \right]^2 - 1 \right\}^{-1/2} dr \tag{S12}$$

By tuning the contact angle and the liquid coating thickness, different bead sizes and shapes can be obtained, as demonstrated in Figure S3.

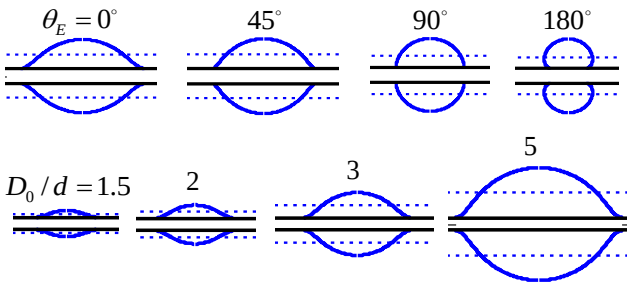

Figure S3. Bead shape tuning. *Simulation of bead shapes with varying liquid-fiber contact angle* θ_E *(upper row) and liquid coating diameter* D_0 *(lower row).*

S3. Bead dimensions and frequency

Equation (S12) can be used to calculate the bead length for given D, d and θ_E. Half the drop length is obtained at $r = D/2$, and therefore the full drop length is:

$$L = 2x(D/2) \tag{S13}$$

a function of D, d and θ_E. This function was fitted to the diameter and length measurements of the epoxy beads (Figure 6 in the main text) with good agreement, where the contact angle served as the fitting parameter ($\theta_E \cong 15°$). Note that the bead length L signifies the contact length between the bead and the fiber, which, for contact angles larger than 90°, is smaller than the maximum bead width (see for example the top-right image in Figure S3).

The distance between adjacent drops (or wavelength) is given by equation (S6):

$$\lambda = \sqrt{2}\pi D_0 \tag{S14}$$

were $D_0 = 2r_0$ is the liquid coating initial diameter (Figure S1), enabling calculation of the drop volume. Assuming no volume loss during drops formation, the volume of a single drop is:

$$v_B = \frac{\pi\left(D_0^2 - d^2\right)\lambda}{4} = \frac{\pi^2}{2\sqrt{2}}\left(D_0^2 - d^2\right)D_0 \tag{S15}$$

This volume can be equated to that obtained by calculating the drop's volume of revolution, using $x(r)$ from equation (S12) and L from equation (S13):

$$v_B = 4\pi \int_{d/2}^{D/2} \left[x(D/2) - x(r)\right] r dr \tag{S16}$$

enabling numerical derivation of D (and subsequently L) as functions of D_0 for given d and θ_E. Consequently, λ can be calculated as a function of D using equation (S14), fitting well the wavelength and diameter measurements of the epoxy beads (Figure 6 in the main text) for $\theta_E = 15°$.

The variables of length dimension in equations (S11)-(S16) can be normalized by the fiber diameter d just by substituting $d = 1$. This allows universal depiction of D/d, L/d and λ/d as functions of D_0/d, with only a single parameter θ_E, plotted in Figure S4. For $\theta_E = 90°$ and thick

coating ($D_0 >> d$), the volume of the drop can be approximated by a sphere having a diameter D, and therefore a good approximation is given by (using equation (S15)):

$$D \cong \sqrt[3]{\frac{6v_B}{\pi}} \cong \sqrt[3]{\frac{3\pi}{\sqrt{2}}} D_0 \cong 1.88 D_0 \qquad \text{(S17)}$$

Because, as seen in Figure S4, the bead diameter is fairly invariable with respect to θ_E, this approximation holds for all values of θ_E. The bead length when $\theta_E = 90°$ can be approximated by $L \cong D$, whereas for other values of θ_E it varies considerably, as seen in the figure.

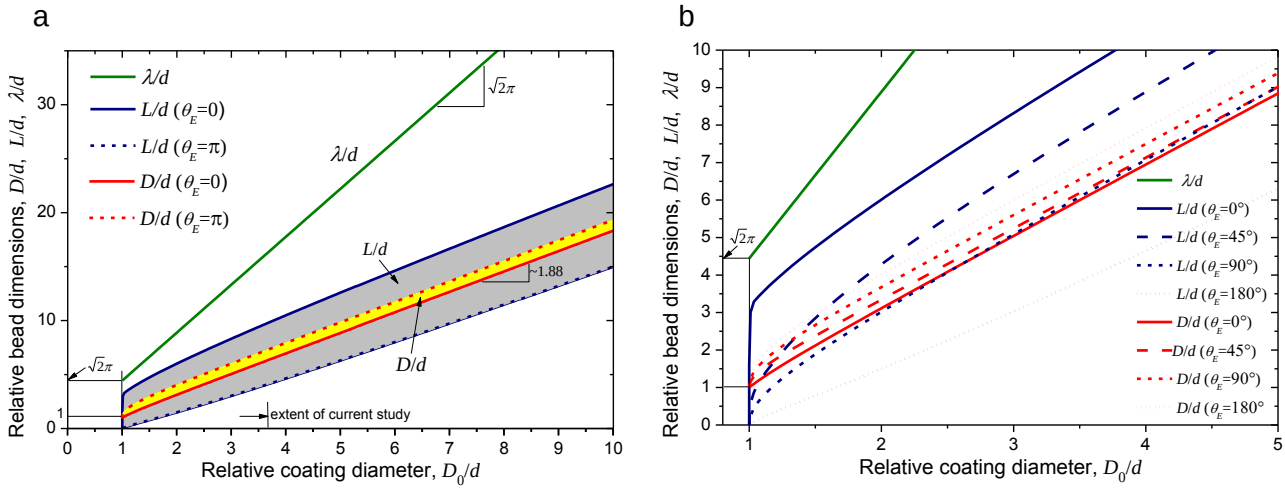

Figure S4. Bead dimensions and frequency. *(a) Simulation of bead diameter* D, *length* L *and wavelength* λ, *against the coating diameter* D_0, *normalized by the fiber diameter* d. *Asymptotic slopes are indicated. The extent of the beads created in the current study is marked. (b) Magnification of (a).*

S4. Beaded fibers volume fraction

As described in the main text (Figure 14a), two tight packing structures are basically possible with beaded fibers: (i) continuous packing, where each bead is in contact with neighboring beads, and (ii) staggered packing, where each bead is in contact with neighboring fibers. These packing structures are depicted below (Figure S5), with their representative unit cells. Other tight packing structures are also possible.

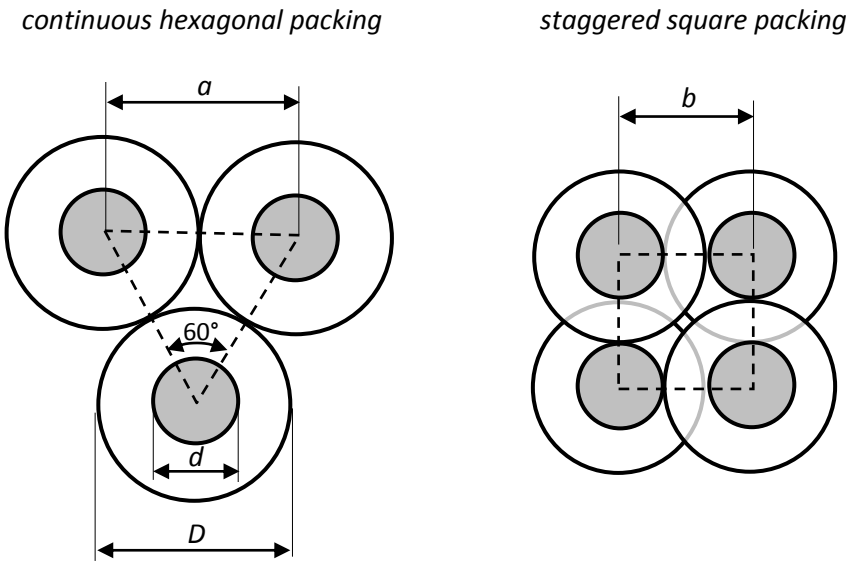

Figure S5. Geometry of beaded fibers tight packing structures. *D and d are the bead and fiber diameters, respectively. The dashed triangle and square represent the unit cell of each packing structure.*

In *continuous packing*, the edge a is equal to the bead diameter D, and therefore the area of the triangular unit cell is $\sqrt{3}D^2/4$. The unit cell contains the area of three 60° circular sections of a fiber, $\pi d^2/8$ in total. The volume fraction is given by the area fraction of the fibers in the unit cell:

$$V_f = \frac{\pi}{2\sqrt{3}}\left(\frac{D}{d}\right)^{-2} \quad \textit{continuous} \tag{S18}$$

In *staggered packing*, the edge b is equal to $(D+d)/2$, and therefore the area of the square unit cell is $(D+d)^2/4$. The unit cell contains the area of four 90° circular sections of a fiber, $\pi d^2/4$ in total. The volume fraction is:

$$V_f = \pi\left(1+\frac{D}{d}\right)^{-2} \quad \textit{staggered} \tag{S19}$$

If the beads get in contact (when $D/d \geq 1/(\sqrt{2}-1) \cong 2.4$), the edge b will be $D/\sqrt{2}$ and V_f will be $\pi(D/d)^{-2}/2$.

The volume fraction in both packing structures converges to $V_f = \pi/(2\sqrt{3}) = 0.907$ (continuous packing) and $V_f = \pi/4 = 0.785$ (staggered packing) for fibers without beads ($D = d$).

References

[1] P.G. de Gennes, F. Brochard-Wyart, D. Quere, Capillarity and wetting phenomena - Drops, Bubbles, Pearls, Waves, Springer-Verlag New York, Inc.2004.

[2] J. Plateau, Statique experimentale et theorique des liquides soumis aux seules forces moleculaires (Experimental and theoretical equilibrium state of liquids subjected to molecular forces only), Gauthiers-Villars, Paris, 1873.

[3] L. Rayleigh, Scientific Papers, (Cambridge: Cambridge University Press, 1899): Proc. London Math. Soc. 10, 4 (1878); Proc. R. Soc. London 29, 71 (1879); Philos. Mag. 34, 145 (1873).